Supporting Information for "The spatial localisation of storm-time ULF waves due to plasmaspheric plumes and implications for calculating radial diffusion"

J. K. Sandhu[1,2], K. R. Murphy[2], I. J. Rae[2], A. W. Degeling[3], A. Osmane[4], D. P. Hartley[5], and L. Olifer[6]

[1]Department of Physics and Astronomy, University of Leicester, Leicester, UK

[2]Department of Maths, Physics and Electrical Engineering, Northumbria University, Newcastle Upon Tyne, UK

[3]Institute of Space Science, Shandong University, Weihai, China

[4]Department of Physics, University of Helsinki, Helsinki, Finland

[5]Department of Physics and Astronomy, University of Iowa, Iowa City, IA, USA

[6]Department of Physics, University of Alberta, Edmonton, AB, Canada

Contents of this file

Introduction This Supporting Information provides further details on aspects of the main manuscript. S1 presents MAGEIS information providing evidence for a drift-resonant interaction between protons and the FLR observed in Event A. S2 includes full details

Corresponding author: J. K. Sandhu, Department of Physics and Astronomy, University of Leicester, Leicester, UK. (jasmine.sandhu@leicester.ac.uk)

on how the radial diffusion coefficients are calculated, using Event D as an illustrative example.

S1. MAGEIS Data Analysis for Event A

To assess whether the $\sim$ 10 mHz signature in the radial magnetic field component is associated with a drift-resonant driven poloidal FLR, we consulted MagEIS observations of energetic ring current protons. Figure S1a shows residual fluxes of 90 degree pitch angle protons at each energy channel, as a function of time. Residual flux, j, is defined as $\frac{j_i - j_0}{j_0}$, where j_i is the differential proton flux at a given time, energy bin, and pitch angle bin, and j_0 is the median flux value over a 10 minute window centred on the sample time and the identical energy and pitch angle bin. This definition of residual flux follows standard usage by (e.g., Claudepierre et al., 2013; Zhao et al., 2021). Each timeseries shown in Figure S1a is bandpass filtered for frequencies between 8 to 12 mHz to focus on frequencies similar to the $\sim$ 10 mHz magnetic field signature. We observe high amplitude periodic fluctuations in the 479 keV protons at $\sim$16:20 UT, with evidence for a phase change between the 479 and 555 keV energy channels (see the timeseries are in anti-phase with each other). Figure S1b shows the amplitude, A, and phase ϕ, of the timeseries for a 10 minute window centred on 16:17 UT. The profiles confirm a clear peak in amplitude accompanied by a $\sim$ 180 degree phase shift at $\sim$ 479 keV. These characteristic features are convincing evidence for drift resonance between the protons and the $\sim$ 10 mHz ULF wave (D. J. Southwood & Kivelson, 1981; Claudepierre et al., 2013).

We apply the drift resonance condition for a 10 mHz wave and a 479 keV proton (D. Southwood et al., 1969) (see Figure S1c). We estimate that the ULF wave has a

wavenumber of approx -100 and is westward propagating, within the typical range of high-m substorm driven ULF waves (Takahashi et al., 1985; Murphy et al., 2018).

If the drift resonance is supporting a fundamental standing Alfvén wave, we can compare the 10 mHz pulsation to the estimated eigenfrequency of the local field line. Using a time-of-flight estimate with the TS04 magnetic field model, and local mass density measurements (EMFISIS electron density and HOPE ion composition (James et al., 2021; Sandhu et al., 2016, 2017)) we estimate the local eigenfrequencies (e.g., Sandhu et al., 2018, 2023). We estimate the fundamental eigenfrequency outside the plume is approximately 20 mHz and inside the plume it is decreased to approximately 4 mHz. The estimates show how the plume density dramatically alters the local eigenfrequency and is therefore capable to excluding the wave interaction from occurring and localises the FLR to the low density region (Zhang et al., 2019). We note that the calculated 20 mHz eigenfrequency is higher than the 10 mHz observed FLR. We attribute the difference to inaccuracies in our eigenfrequency estimates (e.g. choice of field model, assumed field-aligned mass density profile, ion composition estimates). It is outside of the scope to investigate these further, and we provide the eigenfrequency estimates as a approximate guide here.

S2. Estimating Radial Diffusion Coefficients

For a given frequency-resolved measurement of ULF wave power, we can estimate corresponding radial diffusion coefficients, assuming that the wave power value represents the average value across an electron drift orbit. We use the Ozeke, Mann, Murphy, Rae, and Milling (2014) formalism, which represents the magnetic field diffusion coefficient, $D_{\mathrm{LL}}^{\mathrm{B}}$, and the electric field diffusion coefficient, $D_{\mathrm{LL}}^{\mathrm{E}}$, by equations 1 and 2 below. B_E is

the equatorial magnetic field strength at the surface of the Earth, R_E is the radius of the Earth, L is the L-shell, and f is frequency. We can substitute the observed power spectral density for the compressional magnetic field, P_{B}, and azimuthal electric field, P_{E}, into equations 1 and 2 to estimate event-specific diffusion coefficients.

$$D_{LL}^{B} = \frac{L^8 4\pi^2}{9 \times 8 B_E^2} \langle P^B(L,f) f^2 \rangle \tag{1}$$

$$D_{LL}^{E} = \frac{L^6}{8 B_E^2 R_E^2} \langle P^E(L,f) \rangle \tag{2}$$

We now detail how this approach is used to derive the diffusion coefficients presented in the main text. Using Event D as an illustrative example, Figure S2a shows the electron density timeseries through the plume crossing on 24 June 2015 (Event D; Figure 4. Panel (b) shows the timeseries for the total magnetic field power (wine) and total electric field wave power (green) summed over 1 - 15 mHz, and panel (c) shows the location of the spacecraft in L* (indigo) and MLT (rose). The L* value is calculated using the International Radiation Belt Environment Modeling (IRBEM) code (https://sourceforge.net/projects/irbem/) with the Tsyganenko and Sitnov (2005) magnetic field model for an equatorially trapped particle. Figure S2b shows the localised enhancement in magnetic and electric field wave power along the edge of the plume, as discussed in the main text. Note that the y-axis is logarithmic, such that changes are over several orders of magnitude. The width of the power enhancement is roughly estimated by eye and indicated by the grey shaded region in panels (a-d).

Figure S2d,e show the radial diffusion coefficients estimated using the spacecraft ULF wave observations during the enhanced region (rose) and outside the enhancement (in-

digo). The time intervals corresponding to the samples are shown in Table 1. The x-axis shows the L*, and the event-specific diffusion coefficients use the average L* value across the two samples. By estimating the width of the plume, we also show the MLT-averaged radial diffusion (green, see main text for details), where the green and indigo asterisks are almost completely colocated on panels (d,e). We note that we have been relatively conservative when visually identifying the enhanced regions for these events, such that the magnitudes of any differences are assumed to be towards the lower limit.

This approach was extended to all event studies, where the appropriate details are included in Table 1 in the main manuscript.

References

Claudepierre, S. G., Mann, I. R., Takahashi, K., Fennell, J. F., Hudson, M. K., Blake, J. B., ... Wygant, J. R. (2013). Van allen probes observation of localized drift resonance between poloidal mode ultra-low frequency waves and 60 kev electrons. *Geophysical Research Letters*, *40*(17), 4491-4497. Retrieved from https://agupubs.onlinelibrary.wiley.com/doi/abs/10.1002/grl.50901 doi: https://doi.org/10.1002/grl.50901

James, M. K., Yeoman, T. K., Jones, P., Sandhu, J. K., & Goldstein, J. (2021). The scalable plasma ion composition and electron density (spiced) model for earth's inner magnetosphere. *Journal of Geophysical Research: Space Physics*, *126*(9), e2021JA029565. Retrieved from https://agupubs.onlinelibrary.wiley.com/doi/abs/10.1029/2021JA029565 (e2021JA029565 2021JA029565) doi: https://doi.org/10.1029/2021JA029565

Murphy, K. R., Inglis, A. R., Sibeck, D. G., Rae, I. J., Watt, C. E. J., Silveira, M., ...

Nakamura, R. (2018). Determining the mode, frequency, and azimuthal wave number of ulf waves during a hss and moderate geomagnetic storm. *Journal of Geophysical Research: Space Physics*, *123*(8), 6457-6477. Retrieved from https://agupubs.onlinelibrary.wiley.com/doi/abs/10.1029/2017JA024877 doi: https://doi.org/10.1029/2017JA024877

Ozeke, L. G., Mann, I. R., Murphy, K. R., Rae, I. J., & Milling, D. K. (2014). Analytic expressions for ulf wave radiation belt radial diffusion coefficients. *Journal of Geophysical Research: Space Physics*, *119*(3), 1587-1605. Retrieved from https://agupubs.onlinelibrary.wiley.com/doi/abs/10.1002/2013JA019204 doi: https://doi.org/10.1002/2013JA019204

Sandhu, J. K., Degeling, A. W., Elsden, T., Murphy, K. R., Rae, I. J., Wright, A. N., ... Smith, A. (2023). Van allen probes observations of a three-dimensional field line resonance at a plasmaspheric plume. *Geophysical Research Letters*, *50*(23), e2023GL106715. Retrieved from https://agupubs.onlinelibrary.wiley.com/doi/abs/10.1029/2023GL106715 (e2023GL106715 2023GL106715) doi: https://doi.org/10.1029/2023GL106715

Sandhu, J. K., Yeoman, T. K., Fear, R. C., & Dandouras, I. (2016). A statistical study of magnetospheric electron density using the cluster spacecraft. *Journal of Geophysical Research: Space Physics*, *121*(11), 11,042-11,062. Retrieved from https://agupubs.onlinelibrary.wiley.com/doi/abs/10.1002/2016JA023397 doi: https://doi.org/10.1002/2016JA023397

Sandhu, J. K., Yeoman, T. K., James, M. K., Rae, I. J., & Fear, R. C. (2018). Variations of high-latitude geomagnetic pulsation frequencies: A comparison of time-

of-flight estimates and image magnetometer observations. *Journal of Geophysical Research: Space Physics*, *123*(1), 567-586. Retrieved from https://agupubs.onlinelibrary.wiley.com/doi/abs/10.1002/2017JA024434 doi: https://doi.org/10.1002/2017JA024434

Sandhu, J. K., Yeoman, T. K., Rae, I. J., Fear, R. C., & Dandouras, I. (2017). The dependence of magnetospheric plasma mass loading on geomagnetic activity using cluster. *Journal of Geophysical Research: Space Physics*, *122*(9), 9371-9395. Retrieved from https://agupubs.onlinelibrary.wiley.com/doi/abs/10.1002/2017JA024171 doi: 10.1002/2017JA024171

Southwood, D., Dungey, J., & Etherington, R. (1969). Bounce resonant interaction between pulsations and trapped particles. *Planetary and Space Science*, *17*(3), 349-361. Retrieved from https://www.sciencedirect.com/science/article/pii/0032063369900683 doi: https://doi.org/10.1016/0032-0633(69)90068-3

Southwood, D. J., & Kivelson, M. G. (1981). Charged particle behavior in low-frequency geomagnetic pulsations 1. transverse waves. *Journal of Geophysical Research: Space Physics*, *86*(A7), 5643-5655. Retrieved from https://agupubs.onlinelibrary.wiley.com/doi/abs/10.1029/JA086iA07p05643 doi: https://doi.org/10.1029/JA086iA07p05643

Takahashi, K., Higbie, P. R., & Baker, D. N. (1985). Azimuthal propagation and frequency characteristic of compressional pc 5 waves observed at geostationary orbit. *Journal of Geophysical Research: Space Physics*, *90*(A2), 1473-1485. Retrieved from https://agupubs.onlinelibrary.wiley.com/doi/abs/10.1029/JA090iA02p01473 doi: https://doi.org/10.1029/JA090iA02p01473

Tsyganenko, N. A., & Sitnov, M. I. (2005). Modeling the dynamics of the inner magnetosphere during strong geomagnetic storms. *Journal of Geophysical Research: Space Physics*, *110*(A3). Retrieved from https://agupubs.onlinelibrary.wiley.com/doi/abs/10.1029/2004JA010798 doi: https://doi.org/10.1029/2004JA010798

Zhang, S., Tian, A., Degeling, A. W., Shi, Q., Wang, M., Hao, Y., ... Bai, S. (2019). Pc4-5 poloidal ulf wave observed in the dawnside plasmaspheric plume. *Journal of Geophysical Research: Space Physics*, *124*(12), 9986-9998. Retrieved from https://agupubs.onlinelibrary.wiley.com/doi/abs/10.1029/2019JA027319 doi: https://doi.org/10.1029/2019JA027319

Zhao, X. X., Hao, Y. X., Zong, Q.-G., Zhou, X.-Z., Yue, C., Chen, X. R., ... Reeves, G. D. (2021). Origin of electron boomerang stripes: Statistical study. *Geophysical Research Letters*, *48*(11), e2021GL093377. Retrieved from https://agupubs.onlinelibrary.wiley.com/doi/abs/10.1029/2021GL093377 (e2021GL093377 2021GL093377) doi: https://doi.org/10.1029/2021GL093377

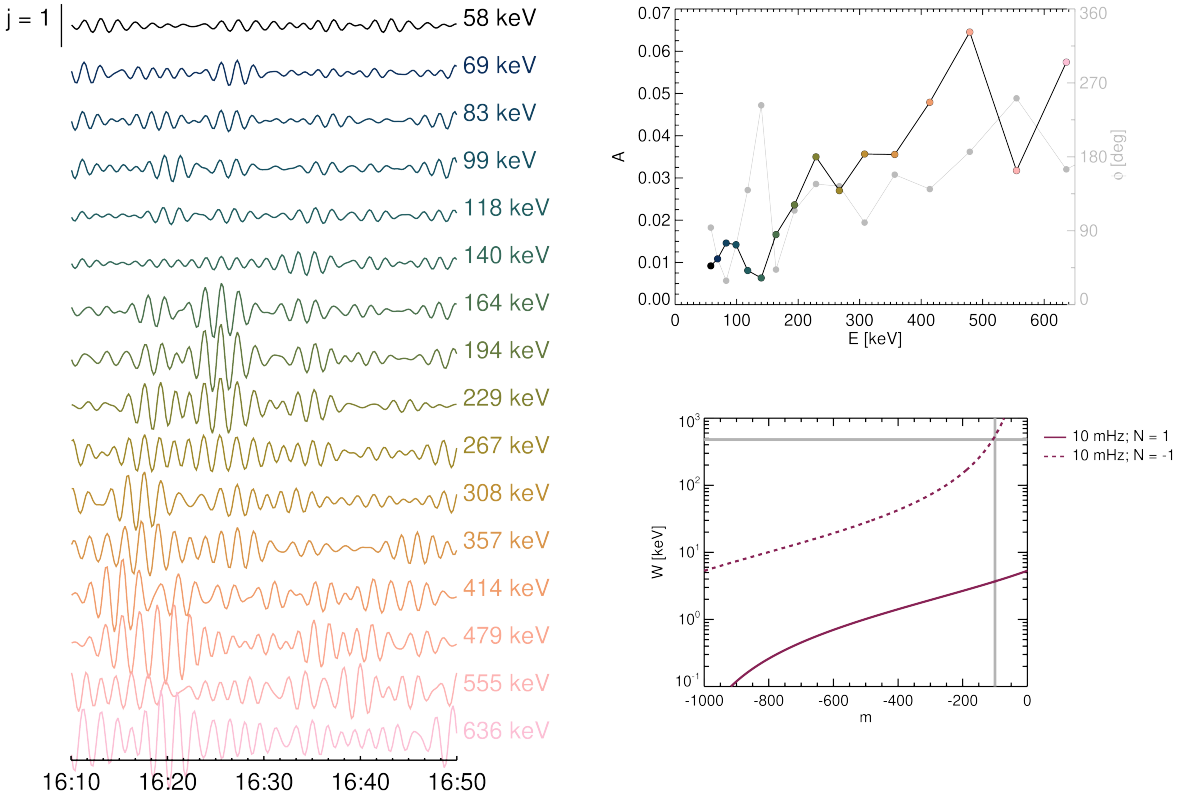

Figure S1. Panel (a) shows the proton residual flux, j, as a function of time for each energy channel, as labelled, between 16:10 to 16:50 24 June 2013. The residual flux has been bandpass filtered for frequencies between 8 to 12 mHz. The amplitude, A, and phase, ϕ [degrees], of the oscillations for each energy channel is shown in panel (b) for a 10 minute window centered on 16:17 24 June 2013. Panel (c) shows the proton energy, $W[keV]$, as a function of wavenumber, m. The solid and dashed purple lines correspond to the resonance condition for a fundamental field line resonance with a frequency of 10 mHz, as labelled. The grey lines map a proton energy of 479 keV to an estimated wave number of approximately -100.

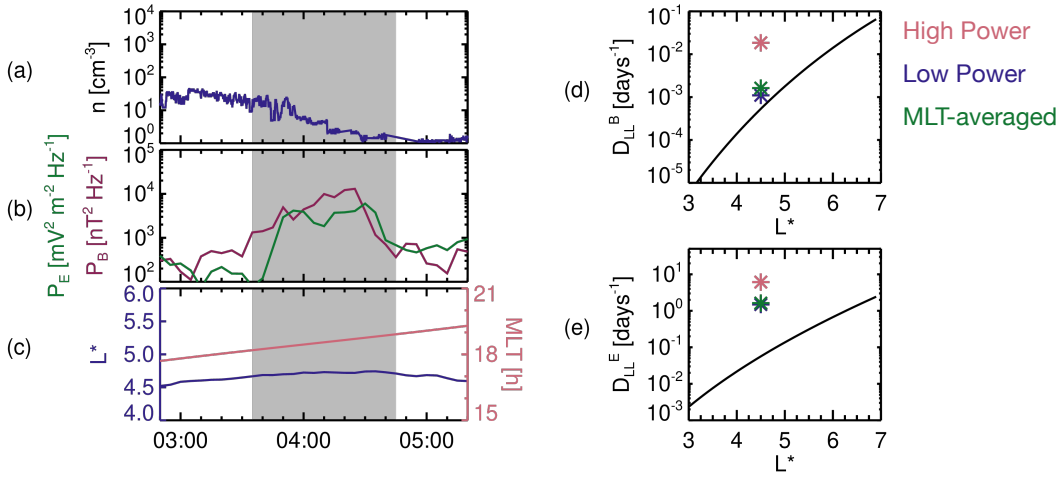

Figure S2. Time series of observations from Van Allen Probe A from 02:50 to 05:20 24 June 2015 is shown in panels (a-c), and panels (d,e) show estimated radial diffusion coefficients based on the observations. Time series are shown for (a) electron density, n [cm^{-3}], (b) power summed over 1 - 15 mHz for the compressional magnetic field (wine) and the azimuthal electric field (green), and (c) the spacecraft position in L* (indigo) and Magnetic Local Time (MLT, rose). Shaded grey regions indicate the interval of enhanced ULF wave power. Panel (d) and (e) show the magnetic radial diffusion coefficient, $D_{\mathrm{LL}}^{\mathrm{B}}$ [days^{-1}], and electric radial diffusion coefficient, $D_{\mathrm{LL}}^{\mathrm{E}}$ [days^{-1}], as a function of L*. The solid black lines correspond to the Ozeke et al. (2014) modelled diffusion coefficients. The rose and indigo asterisks indicate the estimated diffusion coefficients for spacecraft located inside and outside the plume. Panels (d,e) also include green asterisks indicating the estimated MLT-averaged diffusion coefficients, as detailed in the Supplementary Material text.